JOURNAL OF MATERIALS SCIENCE **40** (2005) 6445–6451

Synthesis and characterization of pseudo-ternary $Pb(Fe_{1/2}Nb_{1/2})O_3$-$PbZrO_3$-$PbTiO_3$ ferroelectric ceramics via a B-site oxide mixing route

BIJUN FANG*, YUEJIN SHAN*, KEITARO TEZUKA, HIDEO IMOTO
Department of Applied Chemistry, Faculty of Engineering, Utsunomiya University, 7–1-2 Yoto, Utsunomiya 321-8585, Japan
E-mail: shan@cc.utsunomiya-u.ac.jp
E-mail: fangbj@sohu.com

Published online: 25 October 2005

Perovskite phase formation and dielectric/ferroelectric properties of the pseudo-ternary $Pb(Fe_{1/2}Nb_{1/2})O_3$-$PbZrO_3$-$PbTiO_3$ (PFN-PZ-PT) ferroelectric ceramics have been investigated as promising materials for multi-layer ceramic capacitors. Complete solid solution with pure perovskite phase can be formed in this system in the whole composition range studied using conventional solid-state reaction method via a B-site oxide mixing route. Crystal lattice of the ceramics obtained shrinkages with the increase of the concentration of $Pb(Fe_{1/2}Nb_{1/2})O_3$ (PFN) and expands with the increase of the content of $PbZrO_3$ (PZ). With the increase of the concentration of $PbTiO_3$ (PT), crystal structure of PFN-PZ-PT changes from pseudo-cubic ferroelectric phase to tetragonal one while retains the fraction of PFN as constant. A morphotropic phase boundary (MPB) forms at the composition of 42 mol% PT regardless of whatever concentration of PFN, and the content of PFN affects little on the composition of MPB. The preliminary phase diagram of the PFN-PZ-PT system is determined by X-ray diffraction (XRD) measurements combining with dielectric/ferroelectric characterization. Dielectric measurements indicate that the value of dielectric maximum (ε_m) and the temperature where ε_m appears (T_m) increase with the increase of the concentration of PT. However, PFN exhibits opposite effects, i.e., ε_m increases with the increase of the concentration of PFN accompanied by the decrease of T_m.

1. Introduction

As a result of rapid miniaturization of integrated circuits, multi-layer ceramic capacitors (MLCC) have become increasingly important due to their large capacitance, highly compact design and reliability. Relatively novel lead-based ferroelectrics with complex perovskite structure have been extensively investigated because of their large dielectric constant, relatively low sintering temperature and different types of phase transition [1, 2]. Among which, $Pb(Fe_{1/2}Nb_{1/2})O_3$ (PFN) has been widely used as an important constituent in the MLCC industry, since it exhibits large dielectric constant at a sintering temperature as low as 1000°C [3, 4]. However, PFN exhibits strong frequency dispersion of the dielectric response and relatively large dielectric loss around room temperatures, and the dielectric loss increases rapidly with the increase of temperature, which makes it unsuitable for the application in the MLCC industry. In order to utilize the large dielectric constant and low-temperature sintering capability of PFN, solid solutions of perovskite structure are formed with the addition of other constituents, in which the additives take effects on decreasing the dielectric loss and broadening the temperature characteristic of the dielectric response [5].

Although PFN is a compositionally disordered perovskite ferroelectric, it does not exhibit apparent dispersion of T_m with frequency as is typical for relaxor ferroelectrics. PFN crystallizes into a rhombohedral structure around room temperatures with space group R3m ($a = 4.014$ Å and $\alpha = 89.92°$) and undergoes a diffused phase transition at 112°C to a cubic structure with space group Pm3m ($a = 4.010$ Å) studied on powder compacts [2, 6]. $Pb(Zr_{1-x}Ti_x)O_3$ (PZT) solid solution containing more than 10 mol% $PbTiO_3$ (PT) is ferroelectric which has attracted special attention since MPB forms in this system which divides regions into rhombohedral (the Zr-rich rhombohedral region, containing two ferroelectric phases with space groups R3m and R3c, respectively) and tetragonal (the Ti-rich tetragonal region, with space group P4 mm) structures. Materials around MPB exhibit enhanced dielectric

*Author to whom all correspondence should be addressed.
0022-2461
DOI: 10.1007/s10853-005-1711-7

and electromechanical coupling response which makes PZT so extraordinary, and it has been conjectured that these two features are intrinsically related [7, 8]. Therefore, it is of interest to study the pseudo-ternary $Pb(Fe_{1/2}Nb_{1/2})O_3$-$PbZrO_3$-$PbTiO_3$ (PFN-PZ-PT) ferroelectric solid solution.

However, it is not easy to prepare PFN-PZ-PT with pure perovskite phase since four kinds of cations would occupy the symmetrical crystallographic octahedral cages of the perovskite structure. Since Swartz and Shrout devised a columbite precursor method to synthesize stoichiometric complex perovskite $Pb(Mn_{1/3}Nb_{2/3})O_3$ (PMN) [9], such a technique has been widely used in the synthesis of relaxor ferroelectrics since this method shows substantial improvement in the amount of perovskite phase as compared to the conventional mixed oxide processing [1, 3, 10]. Orita *et al.* developed this technique to a B-site oxide mixing route, where all oxides of the B-site of the perovskite structure were mixed and pre-calcined simultaneously instead of preparing different columbite/wolframite precursors [11]. Such improvement exhibits superior behavior in suppressing pyrochlore phases as compared to the columbite/wolframite precursor method, attributing to the intermediate compounds formed during the pre-calcination of the B-site oxides, which can minimize the preferential reaction of Nb_2O_5 with PbO to form stable pyrochlore phases [2, 4, 5, 11–13]. Therefore, the B-site oxide mixing route was undertaken to synthesize the PFN-PZ-PT ceramics. The feasibility and superiority of the B-site oxide mixing route in the synthesis of complex perovskite ferroelectrics are proven again since the amount of pyrochlore phases in all the ceramics obtained is less than 3 mol%. After repeated pulverization and calcination no pyrochlore phase is detectable.

2. Experimental procedure

PFN-PZ-PT ceramics with nominal compositions xPFN-yPZ-$(1-x-y)$PT (designed as PFN100x-PZ100y-PT100$(1-x-y)$) were prepared by conventional solid-state reaction method via the B-site oxide mixing route since this technique gives a better stabilization of the perovskite structure as compared to the straight calcination or the columbite/wolframite precursor methods [2, 4, 5, 11–13]. The molar fraction of PFN was fixed as 20, 40 and 60 mol%, respectively. The ratio of zirconium to titanium varied from 0.15 to 0.80 at different intervals in order to determine the possible MPB (Fig. 1). High-purity oxides, PbO (>99.9%), Fe_2O_3 (>99.99%), Nb_2O_5 (>99.9%), ZrO_2 (>99.9%) and TiO_2 (>99.9%), were used as raw materials. To maintain stoichiometric the raw materials were dried before weighing and the synthesized B-site precursors were weighed and introduced into the batch calculation.

XRD measurements (Rigaku RINT-2200VS diffractometer) confirmed that there was no free Nb_2O_5 after the mixed B-site oxides were pre-calcined at 1000°C for 4 h. Stoichiometric PbO was added to the synthesized B-site precursors, and the batches were milled and calcined at temperatures between 950 and 1050°C for 2 h. XRD measurements were used to identify the phase formation and repeated pulverization and calcination were untaken if necessary to improve the perovskite phase formation. The perovskite powders obtained were then isostatically pressed into pellets with the addition of 1 wt% polyvinyl alcohol (PVA) binder and sintered at temperatures between 1050 and 1250°C for 2 h. An equiweight of mixed raw oxides with the same composition was used as a lead source in a covered crucible to minimize the volatilization of lead during sintering.

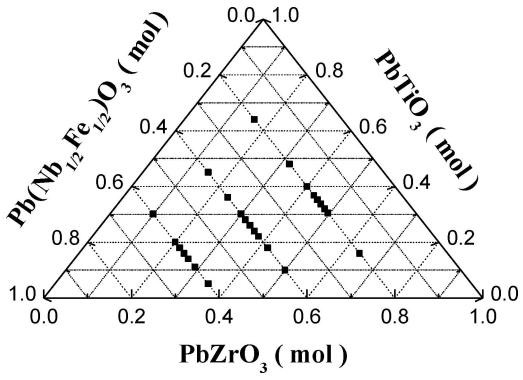

Figure 1 Selected compositions of PFN-PZ-PT investigated in this study.

XRD analysis was carried out on pellets, which confirmed that no additional pyrochlore phase forms during sintering. After polishing to achieve flat and parallel surfaces, apparent bulk density of the sintered PFN-PZ-PT ceramics was measured geometrically. Microstructure morphology of the PFN-PZ-PT ceramics sintered at different temperatures was observed using scanning electron microscope (SEM; Hitachi S-4500) with well-polished specimens. For physical characterization, silver paste was fired on both surfaces of the well-polished pellets as electrodes. The dielectric properties were measured using a computer-interfaced impedance/gain-phase analyzer, under a weak oscillation level (NF Electronic Instruments 2340 LCZ Meter) in the frequency range 100 Hz-1 MHz from room temperature to 800 K. Dielectric hysteresis loops were characterized by a laboratory-modified Sawyer-Tower circuit with a model 10/10B high-voltage amplifier (Trek Inc.). Specimens were immersed in silicon oil to prevent arcing.

3. Results and discussion

The B-site oxide mixing route exhibits superior behavior in the synthesis of complex perovskite ferroelectrics. The amount of $Pb_3Nb_4O_{13}$-type pyrochlore phases is less than 3 mol% in all the PFN-PZ-PT ceramics fabricated by this technique. After repeated pulverization and calcination no pyrochlore phase is detectable by XRD measurements. The success of the B-site oxide mixing route in suppressing pyrochlore phases can be attributed to the intermediate compounds formed after pre-calcination [2, 4, 5, 11–13]. XRD patterns of the B-site precursors show that the main phase

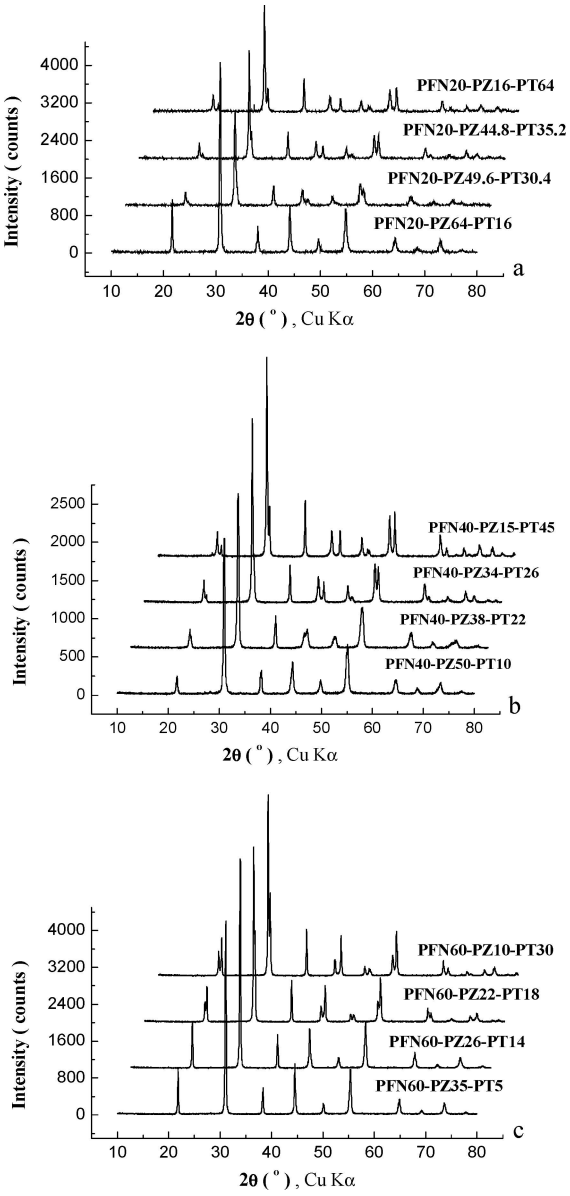

Figure 2 XRD patterns of the PFN-PZ-PT ceramics synthesized via the B-site oxide mixing route. (a) PFN20 system and (b) PFN40 system with repeated calcination; and (c) PFN60 system without repeated calcination.

is some kind of solid solution formed by $FeNbO_4$ and $ZrTiO_4$ corresponding to JCPDS files 16–358 and 34–415, respectively. Although the diffraction peaks are slightly broader and the background is slightly noisier as compared to those of the $FeNbO_4$ precursor in the wolframite precursor method in the fabrication of the $Pb(Fe_{1/2}Nb_{1/2})O_3$ ceramics, no any trace of free Nb_2O_5 (JCPDS files 27-1311 and 37-1468) retains in the B-site precursors. Such results minimize the preferential reaction of Nb_2O_5 with PbO to form stable pyrochlore phases and interpret the superior behavior of this technique as compared to the columbite/wolframite precursor method. Fig. 2 shows XRD patterns of the PFN-PZ-PT ceramics synthesized by this technique with or without repeated calcination, where the development of continuous perovskite solid solutions is well demonstrated. The purity of the perovskite phase is virtually complete, thus the effectiveness of the B-site oxide mixing route in the synthesis of complex perovskite ferroelectrics is proven.

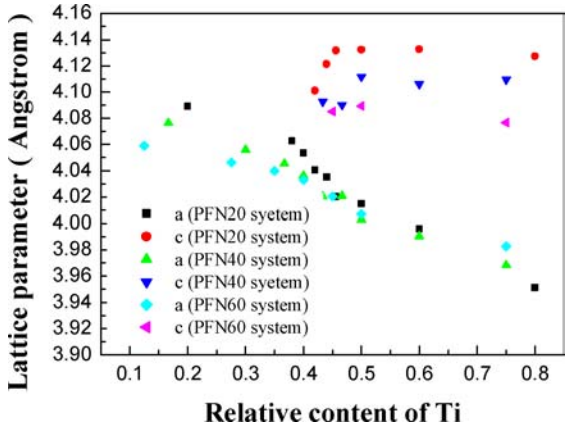

Figure 3 Variation of the lattice parameters as a function of composition of the PFN-PZ-PT perovskite ceramics.

XRD measurements indicate that PFN has a tendency to stabilize the perovskite structure in the PFN-PZ-PT system. The amount of perovskite phase formed increases with the increase of the concentration of PFN. When the content of PFN exceeds 60 mol%, pure perovskite phase forms and repeated calcination is not needed. Crystal structure of the ceramics obtained changes from tetragonal to pseudo-cubic ferroelectric structures with the increase of the ratio of Zr/Ti regardless of the concentration of PFN. The MPB is supposed to locate at the ranges of 0.58–0.60 of the ratio of Zr/Ti for the PFN20 system, 0.567–0.60 for the PFN40 system and 0.55–0.60 for the PFN60 system (according to the formula APFN-(1−A)[*x*PZ-(1−*x*)PT]), respectively, determined by XRD measurements combining with dielectric/ferroelectric characterization. The concentration of PFN exerts little effect on the composition of MPB in the PFN-PZ-PT system, which is beyond our expectation. Since the compositions studied are limited, the exact composition of MPB should be narrower.

Rhombohedral structure is expected to occur at certain ratio of Zr/Ti. However, the small rhombohedral distortion cannot be determined by our XRD analysis with the data recorded continuously in 2θ steps of 0.020°, since the typical full-width-at-half-maximum (FWHM) of the diffraction peaks is 0.15–0.25°. Therefore, the rhombohedral perovskite diffraction peaks are indexed on a pseudo-cubic unit cell. The variation of lattice parameters as a function of composition of the PFN-PZ-PT ceramics is shown in Fig. 3, calculated by the least-squares method using high-angle diffraction peaks. (The coordinate unit of abscissa axis is set according to the formula APFN-(1−A)[*x*PZ-(1-*x*)PT], in which the total amount of zirconium and titanium is regarded as unity. Such setting of the abscissa axis is also used in Figs 4 and 8.) The concentration of PFN influences the cell constants of the PFN-PZ-PT ceramics obtained peculiarly: *a* cell parameter changes little accompanied by the linear decrease of *c* cell parameter with the increase of the concentration of PFN in the tetragonal region; in the pseudo-cubic region, the lattice parameters decrease slightly with the increase of the content of PFN. The ratio of Zr/Ti exhibits different effects on the lattice parameters: *a* cell constant

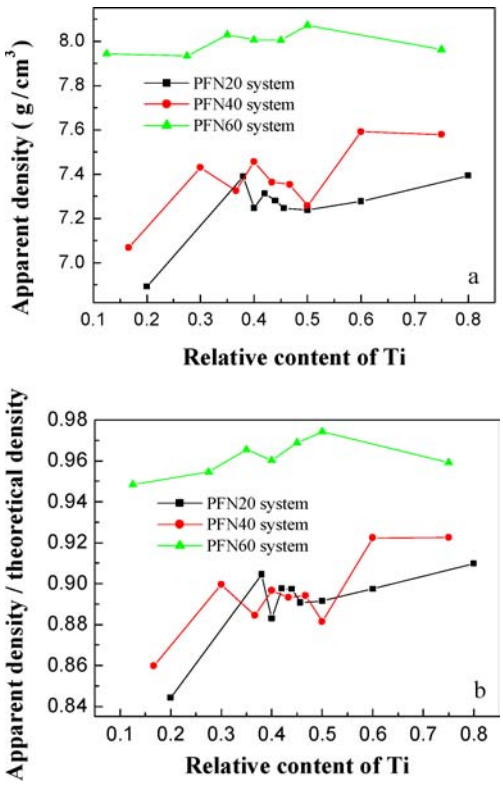

Figure 4 Apparent bulk density (a) and the ratios of the apparent densities to their respective theoretical densities (b) of the PFN-PZ-PT ceramics sintered at 1175°C for 2 h.

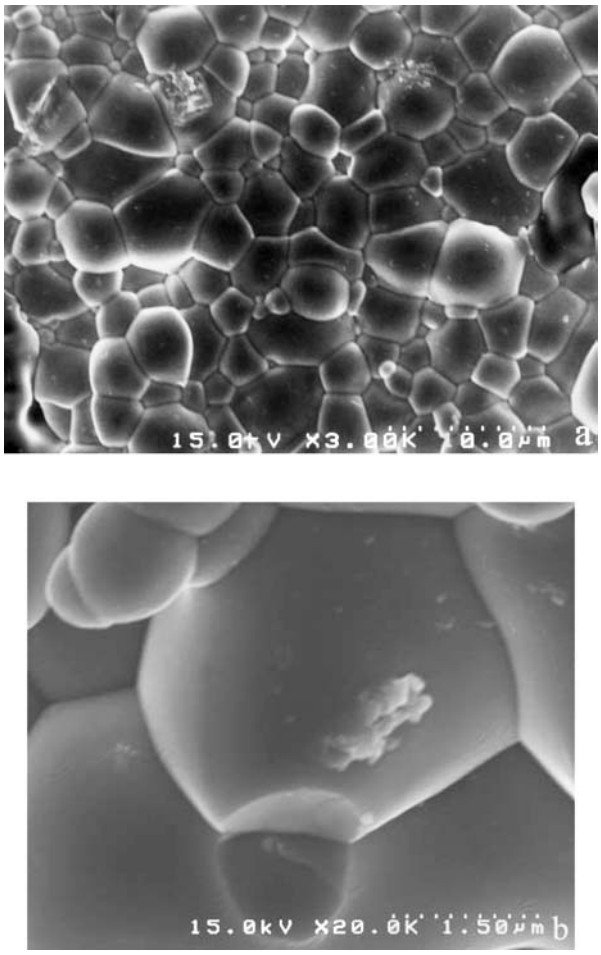

Figure 5 SEM images showing the grain microstructure morphology at (a) 3000 and (b) 20000 magnification of the PFN40-PZ34-PT26 ceramics sintered at 1175°C for 2 h.

increases linearly with the increase of the concentration of PZ across the MPB regions, while *c* cell parameter shows little dependence on the ratio of Zr/Ti in the tetragonal region until to the compositions around MPB where it decreases sharply.

A technological important problem associated with the processing of the lead-based ferroelectrics is the control of evaporation of PbO during sintering stage, since the evaporation of lead produces A-site vacancies and leads to the decomposition of perovskite into pyrochlore phases, which deteriorates physical properties. The technique of the B-site oxide mixing route exhibits a superior behavior in suppressing the evaporation of raw materials since the weight loss during sintering stage is relatively low. The appropriate sintering temperature is determined based on the analysis of weight loss, bulk density and physical properties. In general, with the increase of sintering temperature grains grow up and weight loss increases, which produces large dielectric constant. However, too high sintering temperature does not favor the occurrence of perovskite phase as a consequence of the loss in volatile PbO and results in the formation of pyrochlore phases. Furthermore, higher sintering temperatures associate with larger values of dielectric loss, which is generally regarded as disadvantages in the majority of electronic applications. Apparent bulk density of the sintered PFN-PZ-PT ceramics varies with sintering temperature and the maximum density occurs under sintering temperature between 1160 and 1200°C depending on the concentration of PFN. The variation of density is considered as relating to the weight loss induced by evaporation, the elimination of porosity, the grain-size growth and distribtution, and the densification of ceramics with the increase of sintering temperature, which is confirmed by the SEM images.

Apparent bulk density and the ratios of the apparent densities to their respective theoretical densities of PFN-PZ-PT as a function of composition and the typical SEM microphotographs of the PFN40-PZ34-PT26 ceramics sintered at the optimized temperature 1175°C for 2 h are shown in Figs 4 and 5, respectively. The bulk density increases greatly with the increase of the fraction of PFN, especially when the concentration of PFN exceeds 50 mol%. Such phenomenon can be ascribed to the low-temperature sintering capability of PFN. Increase the amount of PFN not only enhances the densification of the PFN-PZ-PT ceramics (as shown in Fig. 4b, the PFN60 system ceramics exhibit large apparent densities accompanied by high relative densities, i.e., the high ratios of the apparent densities to their respective theoretical densities, exceeding 95% of their respective theoretical densities in the same sintering conditions), but also decreases sintering temperature while still obtains high enough relative density. The ratio of Zr/Ti influences the apparent density differently. Maximum bulk density tends to occur at certain composition in the PFN-PZ-PT ceramics synthesized by the same conditions, which cannot be interpreted by the micro-morphological observation.

The sintered PFN-PZ-PT ceramics exhibit similar micro-morphology. With the increase of sintering

temperature, grains grow up, porosity eliminates gradually, and microstructure becomes dense as indicated by grains packing, which increases the bulk density and the strength of ceramics. PFN-PZ-PT synthesized at the optimized synthesis conditions exhibits a rather homogeneous microstructure and no enclosed pores remain as shown in the SEM images, which proves the feasibility and superiority of the B-site oxide mixing route in the synthesis of complex perovskite ferroelectrics. The scraps attaching to the grains shown in the higher magnification SEM image (Fig. 5b) may be glass phases introduced during the polishing process for preparing the SEM samples.

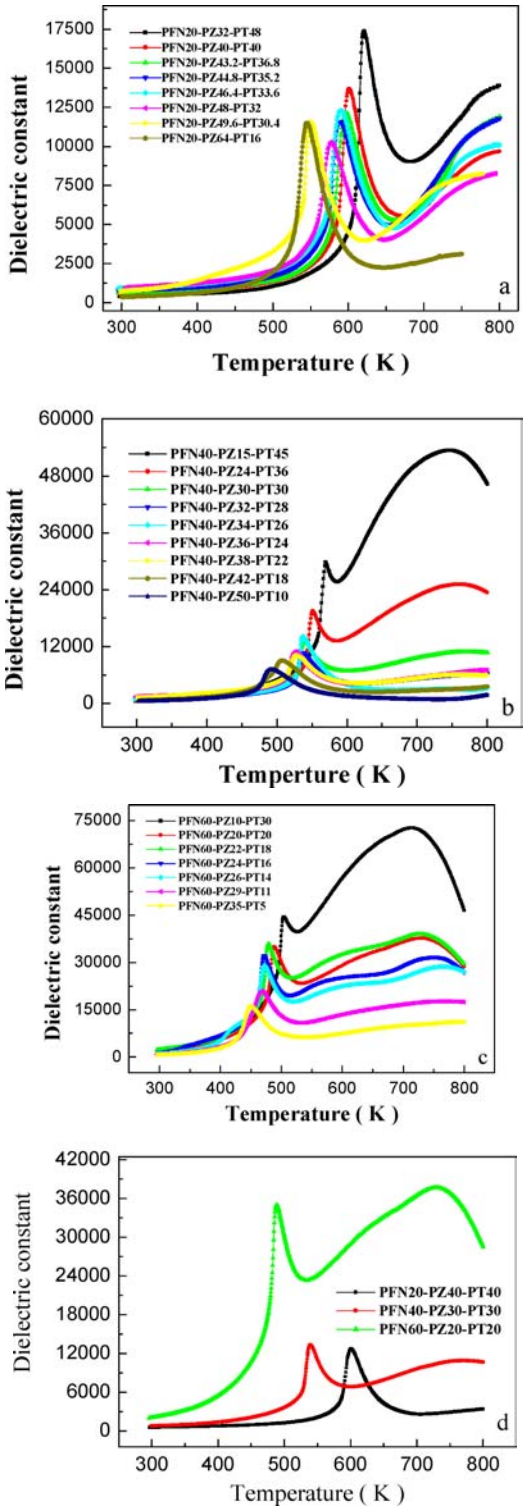

Figure 6 Dielectric properties of the PFN-PZ-PT ceramics sintered at 1175°C for 2 h upon heating. Temperature dependence of the dielectric constant of the (a) PFN20 system ceramics measured at 10 kHz; (b) PFN40 system ceramics measured at 100 kHz; (c) PFN60 system ceramics measured at 100 kH; and (d) Influence of the concentration of PFN on the dielectric behavior of PFN-PZ-PT at fixed 1:1 ratio of PZ/PT measured at 100 kHz.

The typical dielectric behavior of the PFN-PZ-PT ceramics measured at different frequencies is shown in Fig. 6. The dielectric anomalies can be attributed to the phase transition from tetragonal/pseudo-cubic ferroelectric phase to cubic paraelectric phase depending on composition. Such a phenomenon is called the "critical slowing down" and is common in a ferroelectric system near the phase transition point. With the increase of the amount of PZ ε_m and T_m decrease gradually accompanied by the slight broadening of the dielectric peaks. PFN exerts significant effects on the dielectric properties of the PFN-PZ-PT ceramics, where the dielectric peaks broaden greatly accompanied by the increase of ε_m with the increase of the concentration of PFN (as shown in Fig. 6d for various concentration of PFN with fixed 1:1 ratio of PZ/PT). Apparently frequency-dependent dielectric behavior accompanied by slightly large dielectric loss is observed at temperatures around and below T_m when the amount of PFN exceeds 40 mol%. Although ε_m varies around the MPB compositions, enhanced dielectric and electromechanical coupling response are not apparent as usually observed in many other relaxor-based ferroelectrics [7, 8, 14].

The dielectric behavior of the PFN-PZ-PT ceramics obeys the Curie-Weiss law just in a narrow temperature range of the paraelectric region when the concentration of PFN is low. With the increase of the content of PFN, the dielectric behavior deviates the Curie-Weiss law greatly; furthermore, the quadratic law proposed by Uchino *et al*. also cannot fit this dielectric behavior [15]. Such anomalous phenomena accompanied by the strong frequency dispersion of the dielectric response, the relatively large dielectric loss (especially with large concentration of PFN), and the abnormally rapid increase of dielectric constant in the paraelectric region are considered as relating to the nature of the iron-containing compounds, which is usually observed in lossy ferroelectrics, particularly iron-containing compounds [5, 12, 13]. Existence of residual $FeNbO_4$ in the sintered PFN-PZ-PT ceramics is possible although XRD measurements detect no impurity, which exhibits semi-conductive properties and could be responsible for the frequency dispersive behavior and the large value of dielectric loss [16]. Another mechanism deserving consideration correlates with the partial reduction of Fe^{3+} to Fe^{2+} ions during sintering, which is highly sensitive to sintering temperature. Using the Kröger-Vink symbolism, the defect reaction can be written as:

$$Fe_{Fe}^{\times} \rightarrow Fe_{Fe}^{\prime} + h^{\bullet} \qquad (1)$$

The co-existence of Fe^{3+} and Fe^{2+} cations on the equivalent crystallographic sites gives rise to finite

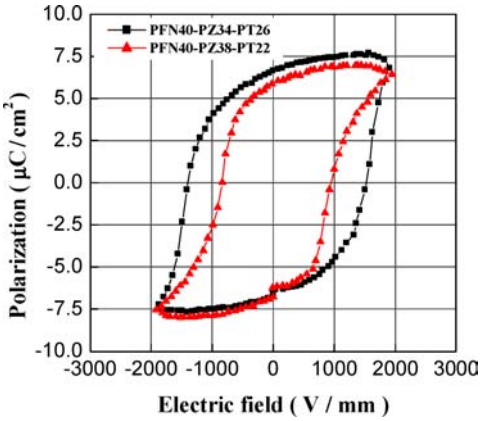

Figure 7 Typical P-E hysteresis loops of the PFN-PZ-PT ceramics sintered at 1175°C for 2 h using the PFN40-PZ34-PT26 (tetragonal structure) and PFN40-PZ38-PT22 (rhombohedral structure) ceramics as examples.

hopping/jump type of conduction mechanism, tending to take effect at lower frequencies. Such mechanism affords thermally activated space-charge polarization conduction [5, 13], which can be reduced significantly by the addition of small amounts of manganese oxide or lithium carbonate [17–19].

Typical dielectric hysteresis loops driven by a 5 Hz sinusoidal electric field are shown in Fig. 7 using the PFN40-PZ34-PT26 and PFN40-PZ38-PT22 ceramics as examples, which crystallize into tetragonal and pseudo-cubic structures respectively. P-E hysteresis loops of the PFN-PZ-PT ceramics exhibit similar patterns in which the polarization may not saturate due to the existence of large magnitudes of space charges and the relatively small electric field used in this experiment. PFN-PZ-PT with tetragonal structure exhibits slightly large remanent polarization and rather rectangular patterns of the P-E hysteresis loops, which can be attributed to the easy movement of the tetragonal ferroelectric domains under external electric field along the spontaneous polarization direction.

Based on above discussion, phase compositions of the pseudo-ternary PFN-PZ-PT system is plotted in Fig. 8, determined by XRD measurements combining with dielectric/ferroelectric characterization. Variation of ε_m as a function of composition of PFN-PZ-PT measured at 10 kHz is shown in the inset. It shows that ε_m increases sharply with the increase of the concentration of PFN, accompanied by the decrease of T_m correspondingly. While keeping the concentration of PFN as a constant, ε_m and T_m decrease gradually with the increase of the content of PZ. Fluctuation of ε_m is observed around the compositions of MPB, but no astonishingly enhanced dielectric response appears as expectation.

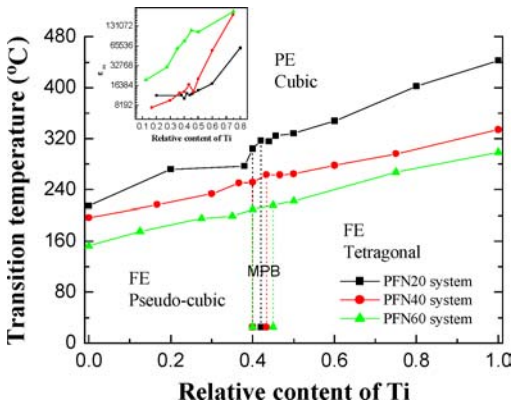

Figure 8 Preliminary phase diagram of the pseudo-ternary PFN-PZ-PT system determined by XDR measurements combining with dielectric/ferroelectric characterization. (The end compositions are linearly extrapolated from the curves.) The dotted curves indicate hypothetical phase boundaries. Variation of ε_m as a function of composition is shown in the inset.

4. Conclusions

Pseudo-ternary $Pb(Fe_{1/2}Nb_{1/2})O_3$-$PbZrO_3$-$PbTiO_3$ (PFN-PZ-PT) ferroelectric ceramics have been synthesized by conventional solid-state reaction method via the B-site oxide mixing route. XRD measurements confirm that complete solid solution of pure perovskite phase can be formed in this system in the whole composition range studied. Crystal structure of the ceramics obtained changes from pseudo-cubic ferroelectric phase to tetragonal one with the increase of the concentration $PbTiO_3$ regardless of the amount of $Pb(Fe_{1/2}Nb_{1/2})O_3$ (PFN) accompanied by the increase of ε_m and T_m as well. With the increase of the concentration of PFN not only the stability of perovskite phase of the PFN-PZ-PT ceramics enhances and the sintering capability of this system improves, but also ε_m increases greatly accompanied by the decrease of T_m.

Acknowledgements

The authors would like to thank the Satellite Venture Business Laboratory of Utsunomiya University, Japan, for financial support.

References

1. T. R. SHROUT and A. HALLIYAL, *Am. Ceram. Soc. Bull.* **66** (1987) 704.
2. R. M. V. RAO, A. HALLIYAL and A. M. UMARJI, *J. Am. Ceram. Soc.* **79** (1996) 257.
3. Y.-C. LIOU, C.-Y. SHIH and C.-H. YU, *Jpn. J. Appl. Phys. Part 1.* **41** (2002) 3829.
4. J.-R. KWON, K.-S. KOH and W.-K. CHOO, *Ferroelectrics* **127** (1992) 161.
5. K. B. PARK and K. H. YOON, *ibid.* **145** (1993) 195.
6. V. A. BOKOV, I. E. MYL'NIKOVA AND G. A. SMOLENSKII, *Sov. Phys. JETP/Acad. Sci. USSR* **15** (1962) 447.
7. B. JAFFE, R. S. ROTH and S. MARZULLO, *J. Appl. Phys.* **25** (1954) 809.
8. B. NOHEDA, J. A. GONZALO, L. E. CROSS, R. GUO, S.-E. PARK, D. E. COX and G. SHIRANE, *Phys. Rev. B* **61** (2000) 8687.
9. S. L. SWARTZ and T. R. SHROUT, *Mater. Res. Bull.* **17** (1982) 1245.
10. D. J. VOSS, S. L. SWARTZ and T. R. SHROUT, *Ferroelectrics* **50** (1983) 203.
11. M. ORITA, H. SATOH, K. AIZAWA and K. AMETANI, *Jpn. J. Appl. Phys. Part 1.* **31** (1992) 3261.
12. B.-H. LEE, K.-K. MIN and N.-K. KIM, *J. Mater. Sci.* **35** (2000) 197.
13. S.-G. JUN and N.-K. KIM, *Mater. Res. Bull.* **34** (1999) 613.
14. C.-S. TU, C.-L. TSAI, V. H. SCHMIDY, HAOSU LUO and ZHIWEN YIN, *J. Appl. Phys.* **89** (2001) 7908.

15. K. UCHINO and S. NOMURA, *Ferroelectrics Lett.* **44** (1982) 55.
16. S. ANANTA and N. W. THOMAS, *J. Eur. Ceram. Soc.* **19** (1999) 1873.
17. T. R. SHROUT, S. L. SWARTZ and M. J. HAUN, *Am. Ceram. Soc. Bull.* **63** (1984) 808.
18. M. P. KASSARJIAN, R. E. NEWNHAM and J. V. BIGGERS, *ibid.* **64** (1985) 245.
19. C. C. CHIU and S. B. DESU, *Mater. Sci. Eng. B* **21** (1993)26.

Received 9 January
and accepted 26 April 2005